Effects of Hyaluronic Acid on MDA-MB-231 Breast Cancer cells

Amber Allen

Abstract

Hyaluronic acid is a crucial part of the extracellular matrix and is involved in the development of cancer. Although HA is well known for its role in tissue hydration and cell proliferation, its effects on breast cancer cells are still being studied. With the focus of this study being on invasion, migration, apoptosis, and proliferation, this study examines how HA affects the behavior of breast cancer cells. Apoptotic marker expression, wound healing assays, and cell viability assays were used to examine the responses of breast cancer cells treated with different doses of HA using in vitro experiments. The study points to a dose dependent interaction, showing that HA inhibits cell growth at higher doses while promoting it at lower ones. Also, HA affected the pathways leading to cell migration and apoptosis, highlighting its dual function in tumor development. These results advance our knowledge of HA's potential as a therapeutic target or risk factor for the treatment of breast cancer. The molecular mechanisms behind these effects and their potential clinical outcome require more investigation.

Key Terms:

- Hyaluronic acid
- Breast cancer
- Apoptosis
- Assays
- Vitro

Introduction

Breast cancer is a serious illness that significantly endangers women's health and can even be fatal. In recent years, extensive efforts have been made to develop effective treatments for this disease. Despite progress in detection and therapy, the molecular mechanisms driving tumor spread remain not fully understood.

One major issue preventing treatment success is the cancer's ability to metastasize and its potential for recurrence (Li et al., 2017). Metastasis often undermines the effectiveness of chemotherapy in treating breast cancer (Li et al., 2017), and nearly all fatal breast cancer cases are linked to metastasis (Jena et al., 2018). Metastasis involves a series of steps, including cell detachment, invasion, and cell proliferation (Li et al., 2017). Cancer cells also have the ability to change the extracellular matrix to start metastasis (Biomedres). The epithelial-mesenchymal transition (EMT) marks the initial step in metastasis and involves various transcription factors (Jena et al., 2018).

To prevent metastasis and recurrence, some strategies have focused on controlling tumor growth at metastatic sites (Nathanson et al., 2021). Another approach targets the extracellular matrix (ECM), which can act as a physical barrier with self-protective properties to restrict tumor spread (Li et al., 2017).

The tumor microenvironment plays a central role in cancer progression. Within this environment, the extracellular matrix is critical because it provides structural support and modulates cell signaling, adhesion, and mechanotransduction (Jena et al., 2018). ECM remodeling is a key process that regulates cancer invasion and metastasis. Matrix metalloproteinases (MMPs) including MMP-2, MMP-9, MMP-11, and MMP-14 play vital roles in degrading matrix proteins, thereby enabling tumor cells to spread (Jena et al., 2018).

A major component in the ECM that can play a key role in cancer growth is Hyaluronic Acid (HA) (Biomedres). HA is a hydrophilic mucopolysaccharide commonly located within the interstitial spaces of animal tissue (Biomedres). Structurally it is a high molecular weight glycosaminoglycan composed of repeating disaccharide units of beta-4- glucosamine (Biomedres). HA has a role in connective tissue but beyond its structural functions, recent studies have demonstrated that HA is actively involved in regulating various cellular processes, including cell differentiation, proliferation, adhesion, migration, and growth (Biomedres).

Many studies have shown that HA can be degraded into smaller fragments after it binds to CD44, which is a HA receptor on the cell surface (Chen et al.,2018). This binding is located at the N-terminal region of the extracellular domain (Chen et al., 2018) This causes a low weight HA, which can accumulate in various types of cancer (Biomedres). This low weight HA can decrease ECM density and make cancer invasion easier to spread throughout (Biomedres). The human genome encodes three hyaluronic acid (HAS) isoforms, HAS1, HAS2, and HAS3 (Lokeshwar et al., 2010). Each are responsible for producing HA of multiple molecular weights. Inhibiting or silencing of this gene in tumor cells has been shown to suppress cell proliferation, invasion, motility in vitro, as well as reduce tumor growth and metastasis in vivo (Lokeshwar et al., 2010).

4-Methylumbelliferone (4-MU) inhibits HA with choleretic and anti-spasmodic properties (Lokeshwar et al., 2010). In mammalian cells, hyaluronic acid (HA) is synthesized by hyaluronic acid synthases (HAS) using UDP-glucuronic acid (UGA) and UDP-N-acetyl-D-glucosamine as precursors (Lokeshwar et al., 2010). UGA is generated through the action of UGA-transferase, which transfers UDP to glucuronic acid (Lokeshwar et al., 2010). However, in cells treated with 4-methylumbelliferone (4-MU), UGA-transferase instead transfers glucuronic acid to 4-MU, reducing the availability of intracellular UGA (Lokeshwar et al., 2010). This depletion of UGA ultimately inhibits HA synthesis (Lokeshwar et al., 2010). Currently the effects of 4-MU involved with inhibiting HA for antitumor intracellular signaling are unknown.

This study aims to study the effects of 4-MU on HA in breast cancer cell type MDA-MB-231. This could potentially result in finding novel anticancer drug targets. Antitumor activity was evaluated through the process of scratch assay which will evaluate cell migration, and hemocytometry to show cell growth and death. It is expected that treatment with 0.6mM 4-MU in a timeframe of 0 to 72 hours will reduce breast cancer cell migration and proliferation while increasing cell death. These effects are likely mediated through the downregulation of cyclin D1 (a proliferation marker) and MMP-9 (a migration marker), alongside the upregulation of caspase 7 (an apoptosis marker).

Methods

Cell Culture and Maintenance

MDA-MB-231 human breast cancer cells were thawed at room temperature with gentle agitation and transferred to a T-75 culture flask containing 25 mL RPMI 1640 medium supplemented with 10% fetal bovine serum (FBS). Cells were incubated at 37°C in a humidified atmosphere containing 5% CO_2. After reaching approximately 60% confluency overnight, the culture medium was aspirated and replaced with fresh RPMI 1640 containing 10% FBS. Cells were allowed to grow until they reached ~95% confluency.

Cells were washed with phosphate-buffered saline (PBS), detached using 2 mL of trypsin-EDTA, and resuspended in 10 mL RPMI with 10% FBS. Following centrifugation at 1000 rpm for 5 minutes, the cell pellet was resuspended in 10 mL of fresh medium. One milliliter of this suspension was diluted in 25 mL of DMEM with 10% FBS and distributed between two new T-75 flasks at a 1:10 split. Remaining cells were pelleted, resuspended in 2 mL RPMI with 10% FBS and 10% DMSO, and stored at –80°C in a controlled rate freezing container.

Cell Plating and Quantification

Once cultures reached ~95% confluency, cells were again detached with trypsin, drawn into a 15 mL conical tube, and centrifuged. The pellet was resuspended in 10 mL RPMI with 10% FBS. A 100 µL portion of the suspension was mixed with 890 µL PBS and 10 µL trypan blue. Ten microliters of this mixture were counted using a hemocytometer to assess cell viability and determine cell density for downstream applications.

Treatment Preparation and Administration

Three treatment groups were prepared:

- **Negative control (0.1% DMSO):** 15 mL RPMI + 10% FBS + 15 µL DMSO
- **Positive control (1% DMSO):** 15 mL RPMI + 10% FBS + 150 µL DMSO
- **4-Methylumbelliferone (4-MU) treatment:** 0.6 mM 4-MU prepared by dissolving 0.12 g powder in 1.13 mL DMSO; 15 µL stock was added to 15 mL RPMI + 10% FBS

Two milliliters of each treatment solution were applied to two wells per group on three 6-well plates after aspirating the original media. Plates were returned to the incubator for exposure.

Serum Starvation and Pre-Scratch Conditions

One 6-well plate reserved for the scratch assay was serum-starved by replacing the media with serum-free RPMI. The following day, cells were dosed with 0.5% FBS RPMI-based formulations:

- **0.1% DMSO:** 5 mL of 0.5% FBS RPMI + 5 µL DMSO
- **1% DMSO:** 5 mL of 0.5% FBS RPMI + 50 µL DMSO
- **4-MU treatment:** 5 mL of 0.5% FBS RPMI + 5 µL of 600 mM 4-MU stock

Scratch Assay Procedure

A scratch was introduced to each well in a vertical line using a sterile p200 pipette tip. Cells were washed gently with PBS to remove debris and then treated with 2 mL of the respective treatment solutions per well. Initial scratch images were captured immediately using a brightfield microscope. Plates were returned to the incubator and imaged again at 24, 48, and 72 hours to monitor wound closure.

Cell Collection and Lysis for Protein Analysis

At each time point (0 h, 24 h, 48 h, and 72 h), selected wells were processed for cell lysis. Cells were washed with PBS, detached with 300 µL trypsin, and collected with 1 mL RPMI + 10% FBS. After centrifugation at 1000 rpm for 5 minutes, cell pellets were resuspended in 500 µL PBS. A trypan blue exclusion assay was performed using a 1:10 dilution of 5 µL cells, 5 µL trypan blue, and 40 µL PBS. Viable cells were counted with a hemocytometer, then lysed with 150 µL RIPA buffer (prepared by combining 2 mL 5x Thermo RIPA buffer, 8 mL distilled water, and 1 protease inhibitor tablet). Lysates were stored at –80°C for further analysis.

ImageJ Analysis of Scratch Assay

Scratch images were analyzed using ImageJ software with the Wound Healing Size Tool plugin. A horizontal reference line was drawn using the straight-line tool. Scale was set globally to 1.8 mm using the *Analyze → Set Scale* function. Each image was cropped to the field of view containing the scratch.

Wound area was calculated using the following plugin parameters: variance window radius = 20, threshold = 10, percent saturated pixels = 0.4, scratch is diagonal selected, and global scale applied. The 24-hour image from well 6 required a threshold adjustment to 20 due to visual variation. Measurements were recorded for each time point.

Results

A scratch assay was performed to evaluate wound closure over 72 hours in MDA-MB-231 cells under three different treatment conditions: 0.1% DMSO (vehicle control), 1% DMSO (positive control), and 0.6 µM 4-Methylumbelliferone (4-MU). Scratch widths were recorded at 0-, 24-, 48-, and 72-hours post-treatment, and average wound sizes were calculated for each group (Table 1). They were shown graphically in Figure 1.

At the initial 0-hour timepoint, the average scratch size for the 0.1% DMSO group was 0.8295 mm^2. This size decreased to 0.274 mm^2 at 24 hours, 0.199 mm^2 at 48 hours, and 0.1485 mm^2 at 72 hours.

The 1% DMSO group began with an average scratch size of 0.9705 mm^2, which reduced to 0.263 mm^2 at 24 hours, 0.149 mm^2 at 48 hours, and 0.138 mm^2 at 72 hours.

The 0.6 µM 4-MU group showed an initial scratch area of 0.8895 mm^2. At 24 hours, the average scratch size was 0.2625 mm^2. By 48 and 72 hours, the wound sizes were 0.23 mm^2 and 0.2405 mm^2, respectively.

Cell growth was assessed using hemocytometer counts for MDA-MB-231 cells treated with 0.1% DMSO (vehicle control), 1% DMSO (positive control), and 0.6 µM 4-Methylumbelliferone (4-MU). Cell counts were recorded at 0, 48, and 72 hours for each treatment group. Average cell numbers are reported in Table 2 and shown graphically in Figure 2.

At the initial 0-hour timepoint, all groups began with an average of 345,000 cells. In the 0.1% DMSO group, cell count increased to 1,070,000 cells at 48 hours and then decreased to 712,500 cells at 72 hours. The 1% DMSO group showed a rise to 956,250 cells at 48 hours, followed by a decrease to 537,500 cells at 72 hours.

In the 0.6 µM 4-MU group, cell growth increased modestly to 604,166.5 cells at 48 hours and declined further to 250,000 cells by 72 hours.

Table 1: Scratch assay

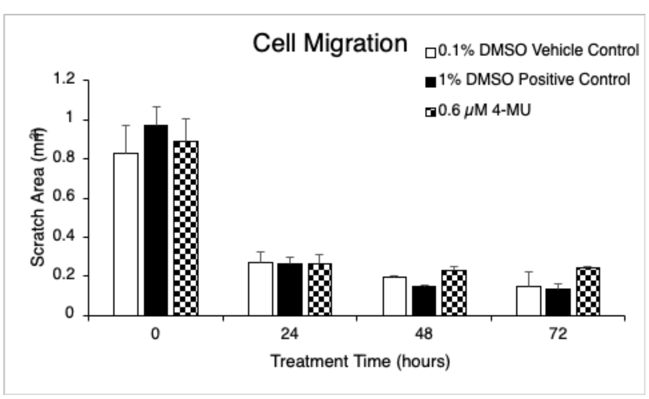

Figure 1: Averages of scratch assay

Time	0	24	48	72
0.1% DMSO Vehicle Control	0.8295	0.274	0.199	0.1485
1% DMSO Positive Control	0.9705	0.263	0.149	0.138
0.6 µM 4-MU	0.8895	0.2625	0.23	0.2405

Figure 2: Cell growth table

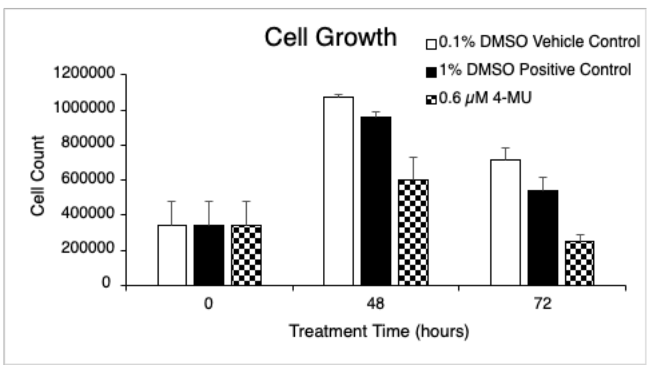

Table 2: Cell growth averages

Time	0	48	72
0.1% DMSO Vehicle Control	345000	1070000	712500
1% DMSO Positive Control	345000	956250	537500
0.6 µM 4-MU	345000	604166.5	250000

Discussion

Based on the scratch assay and hemocytometer data, 4-MU (0.6 µM) clearly reduced both migration and proliferation of MDA-MB-231 breast cancer cells over 72 hours. In the scratch assay, the 0.1% and 1% DMSO control groups constantly closed the wound at a consistent rate by the 72 hours, this was expected for this highly migratory cell line. The 4-MU treated group showed early wound closure by the 24-hour mark but plateaued with minimum closure at 48 and 72 hours.

The hemocytometer counts reflected a similar trend. All groups started with ~345,000 cells, but by 48 hours the controls grew significantly then declined slightly by 72 hours. The 4-MU group showed a small increase at 48 hours and dropped significantly below starting values by the 72-hour mark. These results suggest that 4-MU impacts both movement and growth which are two essential mechanisms in cancer progression.

This aligns with previous findings. Karalis et al. reported that 4-MU suppressed migration, adhesion, and invasion in ER- breast cancer cells, including MDA-MD-231, by targeting HA synthesis and reducing CD44 expression. HAS2, which is highly active in these cells and drives HA production, is also downregulated by 4-MU, leading to reduced HA levels and impaired motility. These mechanisms lead towards understanding why there was limited scratch closure beyond 24 hours.

Additionally, 4-MU's antiproliferative effects have been documented previously. Qin et al. showed that it activates NSMase2, elevates ceramide levels, and downregulates HAS2 and

Akt signaling processes that together inhibit proliferation and even induce apoptosis in tumor cells. This supports the findings in this experiment's hemocytometer data, which shows a declining cell number by the 72-hour mark and suggest that 4-MU does more than just slow growth in may also reduce viability.

The role of HA in supporting cancer cell behavior is increasingly recognized. High HA production and CD44 receptor signaling enhance migration and stem-like properties in aggressive breast cancer lines like MDA-MB-231 (Parnigoni et al., 2024). By interfering with HA synthesis, 4-MU limits these processes, impacting both movement and proliferation (Liu et al., 2024). It also downregulates CD44 and RHAMM receptors, disrupting HA-receptor-mediated (Liu et al., 2024).

Finally, studies like Pibuel et al. show various cancer types from glioblastoma to osteosarcoma report that 4-MU consistently inhibit proliferation, migration, and invasion. This often includes apoptosis or senescence via HA dependent and independent mechanisms. This research solidifies that pattern in triple negative breast cancer cells.

In conclusion, the results of this experiment support ideas that 4-MU disrupts migration and proliferation simultaneously in MDA-MB-231 cells by targeting HA synthesis and downstream pathways like CD44 and Akt. These findings deepen our understanding of 4-MU's anticancer actions and strengthen the understanding for its development as a therapeutic agent against aggressive breast cancer.

Literature Cited

Chen, Chen, et al. "The Biology and Role of CD44 in Cancer Progression: Therapeutic Implications - Journal of Hematology & Oncology." *BioMed Central*, BioMed Central, 10 May 2018, https://jhoonline.biomedcentral.com/articles/10.1186/s13045-018-0605-5?utm

Biomedres, biomedres.us/pdfs/BJSTR.MS.ID.003730.pdf. Accessed 27 June 2025.

Jena, Manoj Kumar, and Jagadeesh Janjanam. "Role of Extracellular Matrix in Breast Cancer Development: A Brief Update." *F1000Research*, U.S. National Library of Medicine, 5 Mar. 2018, https://pmc.ncbi.nlm.nih.gov/articles/PMC6020719/?utm

Jing Li, et al. "Synergistic Inhibition of Migration and Invasion of Breast Cancer Cells by Dual Docetaxel/Quercetin-Loaded Nanoparticles via AKT/MMP-9 Pathway." *International Journal of Pharmaceutics*, Elsevier, 21 Mar. 2017, www.sciencedirect.com/science/article/abs/pii/S037851731730217X?via%3Dihub

Karalis TT; Heldin P; Vynios DH; Neill T; Buraschi S; Iozzo RV; Karamanos NK; Skandalis SS; "Tumor-Suppressive Functions of 4-MU on Breast Cancer Cells of Different ER Status: Regulation of Hyaluronan/Has2/CD44 and Specific Matrix Effectors." *Matrix Biology: Journal of the International Society for Matrix Biology*, U.S. National Library of Medicine, https://pubmed.ncbi.nlm.nih.gov/29673760/ . Accessed 27 June 2025.

Nathanson, S David, et al. "Mechanisms of Breast Cancer Metastasis." *Clinical & Experimental Metastasis*, U.S. National Library of Medicine, Feb. 2022, http://pmc.ncbi.nlm.nih.gov/articles/PMC8568733/

Lokeshwar, Vinata B, et al. "Antitumor Activity of Hyaluronic Acid Synthesis Inhibitor 4-Methylumbelliferone in Prostate Cancer Cells." *Cancer Research*, U.S. National Library of Medicine, 1 Apr. 2010 https://pmc.ncbi.nlm.nih.gov/articles/PMC2848908/

Parnigoni, Arianna, et al. "Effects of Hyaluronan on Breast Cancer Aggressiveness." *MDPI*, Multidisciplinary Digital Publishing Institute, 27 July 2023, https://pmc.ncbi.nlm.nih.gov/articles/PMC10417239/

Pibuel MA; Díaz M; Molinari Y; Poodts D; Silvestroff L; Lompardía SL; Franco P; Hajos SE; "4-Methylumbelliferone as a Potent and Selective Antitumor Drug on a Glioblastoma Model." *Glycobiology*, U.S. National Library of Medicine, https://pubmed.ncbi.nlm.nih.gov/32472122/ Accessed 27 June 2025.

Qin, Jingdong, et al. "The Hyaluronic Acid Inhibitor 4-Methylumbelliferone Is an Nsmase2 Activator-Role of Ceramide in Mu Anti-Tumor Activity." *Biochimica et Biophysica Acta*, U.S. National Library of Medicine, Feb. 2016, https://pmc.ncbi.nlm.nih.gov/articles/PMC4691382/